Title

Integrating Literature Evidence to Enhance CRISPR-based Target Screening for Hand-foot Syndrome

Abstract

Traditional experimental high-throughput screening (HTS) methods, exemplified by CRISPR-based screening techniques, have revolutionized target identification in drug discovery. However, such screens generate expansive and unrelated target lists necessitating costly and time-consuming experimental validation. To address this challenge, we propose a dual-filter strategy that integrates literature-mined targets with CRISPR/Cas9 screening outputs, prioritizing pre-validated candidates in literature to minimize lab validation burden. To validate our dual-filter strategy, we applied it using hand-foot syndrome (HFS), a clinically challenging side effect induced by fluoropyrimidine treatment, as a model. This approach identified ATF4 as a key regulator of 5-FU toxicity in the skin and revealed forskolin as a potential therapeutic agent of HFS. Mechanistically, forskolin alleviates HFS by the induction of MEK/ERK-mediated ATF4 expression, which upregulates IκB through activating the negative feedback loop within the integrated stress response (ISR) pathway. Our findings demonstrate that this dual-filter strategy could significantly accelerate drug discovery by improving target screening efficiency and reducing experimental burden.

Keywords: CRISPR/Cas9, 5-fluorouracil, hand-foot syndrome, ATF4, forskolin

Introduction

Identifying targets for diseases is a critical step in the drug development process. Among them, experimental high-throughput screening (HTS) methods aim to rapidly extract potential targets from large-scale datasets, including genome function studies, genome association studies, transcriptomics, and proteomics. The development of these methods has greatly improved drug development efficiency. Currently, the HTS method has been widely used in target screening in a variety of research fields, including cancer [1], antibiotic discovery[2,3], viral infections[4] and diabetes[5].

However, despite their advantages, screening results from HTS often exhibit high false-positive rates and lack reproducibility[6]. This demands extensive experimental verification of numerous targets to identify the most promising candidates [7], a process that is both costly and time-consuming, consequently augmenting the overall burden of drug development. Therefore, developing approaches to refine screening results and reduce the workload associated with target validation is critical for improving the efficiency of the drug discovery process.

To enhance the accuracy of target identification and reduce the burden of experimental validation, several strategies have been explored. Some studies have limited the functional scope of screened genes by excluding non-relevant genes, such as housekeeping genes[8], or by employing specialized libraries [9,10] before experimental screening. However, these approaches are typically applicable only in specific research contexts. In addition, some researchers have integrated multi-omics databases to refine experimental screening results[9,11]. As omics datasets themselves still originate from

large-scale experimental data, this approach often inherits the same limitations, including suboptimal accuracy in identifying targets.

Furthermore, some researchers have attempted to simulate the manual ranking process of experts by integrating diverse types of evidence, including preclinical, clinical, literature, and gene essentiality data[12]. However, this multi-objective ranking approach, in the absence of mature methods for integrating heterogeneous datasets, may lead to the over-ranking of genes based on high scores in a single criterion. It may also result in insufficient differentiation between high-score genes, making it challenging to identify the most optimal target. Among the mentioned evidence, literature data is widely available across most disease research areas and could provide numerous literature-reported targets, which are generally supported by robust experimental evidence. Integrating literature data with experimental HTS results offers an alternative filtering strategy to reduce the workload of researchers by enabling the substitution of labor-intensive experimental processes with computational validation. Therefore, we established a target screening strategy that employed literature-based screening as the second filter to prioritize experimental HTS outputs.

To evaluate the potential of our strategy in enhancing target screening efficiency, we used hand-foot syndrome (HFS), a common side effect of fluoropyrimidine chemotherapy, as a study case. Capecitabine, a prodrug of 5-fluorouracil (5-FU), is currently known to have the highest risk of inducing HFS among chemotherapy agents[13]. The administration of capecitabine induces a situation where approximately 40% of patients necessitate dose modification[14], with the primary causative factor

being HFS[15]. Although as a dose-limiting side effect, HFS lacks clinical standard and effective management, highlighting the urgent need to discover additional candidate drugs. Furthermore, some therapeutic agents targeting 5-FU toxicity have been shown to have the potential for alleviating HFS. Thymidine diacetate, a prodrug of thymidine, can counteract the inhibitory effect of 5-FU on TS by supplementing thymidine. Local 为了 administration of this drug has demonstrated efficacy in relieving HFS[16]. Uridine can mitigate 5-FU toxicity by increasing the intracellular UTP pool to compete with FUTP, the latter is one of the activated forms of 5-FU, which damages RNA by incorporating it into RNA[17]. 10% uridine ointment has been shown to relieve HFS symptoms[18,19]. These findings support the rationale for identifying the targets regulating 5-FU toxicity in skin to discover agents for relieving HFS.

Genome-wide CRISPR/Cas9 screening technology, known for its robust gene-phenotype causal analysis[20], is commonly employed to identify targets for combination therapies that enhance the sensitivity or reduce the resistance of chemotherapy[21,22]. Through integrating literature-based screening with genome-wide CRISPR/Cas9 screening, we identified ATF4 as a promising target for modulating 5-FU toxicity in the skin. Subsequent efficacy validation of forskolin, an ATF4 inducer, demonstrated its ability to detoxify 5-FU and alleviate HFS. Further exploration of the biological mechanisms underlying forskolin's activation also confirmed the function of ATF4 in regulating 5-FU toxicity. In conclusion, our study presents an effective target screening strategy for drug discovery.

Results

1. Genome-wide CRISP/Cas9 screening identified targets regulating 5-FU toxicity in HaCaT

We conducted genome-wide CRISPR/Cas9 screening on HaCaT cells under 5-FU treatment to identify modulators of 5-FU toxicity in keratinocytes. We selected the Human GeCKOv2 Library A, which targets 19,050 genes, with three sgRNAs per gene, and packaged them into lentivirus. The exogenous DNA embedded with sgRNAs sequence in lentivirus was then transduced to HaCaT cells expressing Cas9 protein at a multiplicity of infection (MOI) of 0.3. Those cells with sgRNAs were selected and amplified with puromycin. The pool of library-transduced cells was divided into three groups: a control group treated with PBS, and two treatment groups exposed to 5-FU separately at IC_{50} (0.0024 μM) and IC_{99} (0.1 μM) concentrations. Each group was cultured under its conditions for 10 days. At the end of experimental screening, the genomic DNA in all groups were sequenced using next-generation sequencing (NGS). Each sgRNA count hit by NGS represents a single cell with a gene knocked out. Sequence data revealed that in group IC_{50} and group IC_{99}, the targeted genes account for 98% of the total genes in the library, and the genes targeted by two or more active sgRNAs comprise 85% and 87%, respectively. Data was analyzed by MAGeCK. The normalized sgRNA counts and robust rank aggregation (RRA)scores are available in separate files (**Table S1, S2**). Finally, we obtained two target libraries, Library-IC_{50} and Library-IC_{99} **(Fig. 1a).**

For either of the two libraries, we distinguished negative and positive screening results by ranking the RRA score. Among Library-IC_{50}, targets with p-value < 0.02 were distinguished into Library-IC_{50}-N (negative screening) and Library-IC_{50}-P (positive screening); among Library-IC_{99}, we also obtained Library-IC_{99}-N and Library-IC_{99}-P. Targets present in both the Library-IC_{50}-P and Library-IC_{99}-P, but absent from all other libraries, were classified into the Library-P group, consisting of 49 genes marked with green dots **(Fig. 1b, c).** In the same way, Library-N contains 45 genes marked with red dots **(Fig. 1b, c).** In addition, we extracted the top 10 targets from the negative or positive screening of Library-IC_{50} and Library-IC_{99} to form Library-Top-N and Library-Top-P, respectively **(Fig. 1d, e)**. In the end, this resulted in two consolidated libraries from CRISPR/Cas9: Library-CR-N, comprising 60 targets, and Library-CR-P, comprising 67 targets **(Fig. 1e)**. Combining the two libraries, we established Library-CR, which includes 127 targets potentially influencing 5-FU toxicity in keratinocytes. All target libraries identified in this study are available in a separate file **(Table S3)**.

2. Text mining screening identified targets regulating 5-FU toxicity in the skin

Our genome-wide CRISPR/Cas9 screening revealed 127 putative genetic modulators associated with 5-FU toxicity, all requiring functional validation through experimental characterization. We conducted a literature screening via text mining technology to identify literature-supported targets related to 5-FU toxicity regulation in order to alleviate the burden of experimental verification by secondly filtering the

CRISPR/Cas9 screening outputs.

However, rare available literature in the field of fluoropyrimidine-induced HFS limited comprehensive text mining. To overcome this challenge, we found an approach to augment available literature by incorporating other research domains related to 5-FU beyond the scope of HFS. The applied 5-FU dosage correlates with its anti-tumor efficacy and the severity of HFS in a similar way. Thus, the genes regulating 5-FU toxicity in cancer cells may have the same impact on the effects of 5-FU in keratinocytes, prompting us to expand the available literature from the domain of HFS to anti-tumor research. In order to leverage available literature from anti-tumor research, we extracted two key parameters pertinent to HFS: the chemotherapeutic drug "5-FU" and the affected tissue "skin", and screened targets from the two aspects separately.

The literature-based targets screening process is shown in **Fig. 2a**. We first conducted a search using the keywords "5-FU AND (resistance OR sensitivity) AND (expression OR silence OR knockdown)" in the PubMed database for the information in title and abstract. By applying the "Tokenizer" program, we segmented the text of title and abstract into individual words, creating a word list. By comparing the word list with the reference gene list, we extracted and recorded the genes contained in the word list using the "Extractor" program. The outputs are the extracted genes reported to be correlative with 5-FU toxicity. The reference gene list including gene symbols and gene aliases is provided by the National Center for Biotechnology Information (NCBI) **(Table S4)**.

Since the genes identified by the "Extractor" are reported in different types of cells and tissues, to ensure the screened targets play a crucial role in skin-limited side effects, we

extracted distinct targets highly expressed in the skin by leveraging the GTEx database, with the median TPM > 10. Finally, the intersection of targets from literature screening and GTEx database yielded to the Library-TM, a target library based on text mining, consisting of 592 genes **(Fig. 2a, Table S5).**

GO enrichment analysis of Library-TM revealed that most enriched gene function terms (top 6 terms) are associated with "response to stimulus" **(Fig. 2b)**. This suggests that the biological processes involved in the cellular response to stimulus may regulate 5-FU toxicity.

3. ATF4 was identified through integrating literature evidence with CRISPR/Cas9 screening

We applied the 592 targets identified through literature-based screening to refine the 127 targets from the CRISPR/Cas9 screening by Library-CR and Library-TM. We identified two genes through the dual-filter strategy, *ATF4* and *MAPK14* **(Fig. 3a)**.

In the CRISPR/Cas9 screening, *ATF4* knockout resulted in a more pronounced change in normalized sgRNA counts than *MAPK14* knockout **(Fig. 3b)**. *ATF4* knockout also exhibited larger potential in regulating 5-FU toxicity with supporting evidence both in statistical significance and fold change **(Fig. 3c)**. Additionally, we also evaluated the performance of *ATF4* and *MAPK14* in literature screening. *ATF4* was reported to enhance 5-FU resistance, whereas *MAPK14* was noted to exert a contradictory capability in regulating 5-FU toxicity. Two in five articles reported its function in enhancing 5-FU sensitivity, which is inconsistent with the CRISPR/Cas9 screening

results **(Fig 3d)**. The regulation of 5-FU toxicity was related to "response to stimulus" as indicated by the top six GO enrichment terms of Library-TM. *ATF4* appeared in five terms, while *MAPK14* in only one term, suggesting a stronger functional link between ATF4 and 5-FU toxicity **(Fig 3e)**. Therefore, as indicated by the CRISPR/Cas9 screening results, *ATF4* holds greater potential than *MAPK14* for modulating 5-FU toxicity.

Our findings confirmed that knockdown and knockout of *ATF4* enhances 5-FU sensitivity in HaCaT cells **(Fig. 3f, g, Fig. S1)**, supporting the role of ATF4 in regulating 5-FU toxicity as suggested by both CRISPR/Cas9 and text mining analyses. Finally, *ATF4* is identified as a candidate gene for modulating 5-FU toxicity.

4. Forskolin reverses 5-FU toxicity in HaCaT as an ATF4 inducer

ATF4 knockdown was indicated to enhance 5-FU toxicity, driving us to discover the agent detoxifying 5-FU through increasing ATF4 expression. Forskolin has been reported to induce ATF4 expression[23], which was also verified in our experiments **(Fig. 4a, Fig. S2, A).** Therefore, forskolin was expected to reverse 5-FU toxicity by upregulating ATF4.

The CCK-8 assay and LDH release assay demonstrated that forskolin treatment reversed 5-FU toxicity to HaCaT cells in a dose-dependent manner **(Fig. 4b, Fig. S2, B)** and significantly increased the IC_{50} of 5-FU in HaCaT **(Fig. 4c)**. As a plant extract, forskolin may exert action through various unknown pathways. This drives us to

explore the role of ATF4 in forskolin-induced 5-FU detoxification. Our results showed that *ATF4* knockout diminished the dose-dependent protection of forskolin **(Fig. 4d, e)** and impaired the increase of 5-FU IC_{50} induced by forskolin **(Fig. 4d, f).** This indicates that ATF4 contributes partially to the detoxification effect of forskolin. The remaining forskolin's effects may derive from other signal pathways downstream of the MEK/ERK activation, but not the induction of ATF4 **(Fig. S2, C)**.

5-FU is known to induce cell or tissue damage by blocking the cell cycle, promoting apoptosis, and increasing the release of pro-inflammatory factors[24-26]. According to our results, forskolin was found to counteract 5-FU's effects on arresting cell cycle **(Fig. 4g)**, inducing apoptosis **(Fig. 4h)**, and upregulating the expression of classical pro-inflammatory factors (IL-6, IL-1β, TNF-α) **(Fig. 4i)**, colony-stimulating factor (GSF-2), and chemokines (CXCL-1) **(Fig. S2, D and E).** These findings suggest that forskolin has the potential to act as a detoxifying agent against 5-FU.

5. Forskolin reverses HFS induced by capecitabine in vivo

In vitro findings demonstrated the ability of forskolin to rescue 5-FU toxicity in HaCaT cells, reflecting its potential to alleviate HFS. We formulated a gel containing 10% forskolin. After daily administration of capecitabine, the gel containing (CAP-FRSK) or not containing (CAP-Vehicle) forskolin was applied topically to the hind paws of rats. The progression of HFS was monitored and assessed using a disease grading system: Grade 1 indicated mild dryness, while Grade 2 represented severe dryness, desquamation, or dryness with redness and swelling. By day 35, since approximately

90% of rats in the CAP-Vehicle group (HFS model group) exhibited Grade 2 HFS, we ended the experiment.

Notably, the severity of HFS in the CAP-FRSK group was significantly lower than the CAP-Vehicle group **(Fig. 5a).** The incidence of severe HFS like Grade 2 HFS during chemotherapy is crucial for the clinical decision of dose modification[27]. Therefore, we analyzed the effect of Forskolin on the incidence of Grade 2 HFS. Our analysis revealed a lower daily proportion of Grade 2 HFS in the CAP-FRSK group, indicating a slower progression of symptoms **(Fig. 5b)**. At the end of the experiment, the incidence rate for Grade 2 HFS during the whole experiment was 91% (n=12) for CAP-Vehicle and only 25% (n=12, one death on day 26) for CAP-FRSK. The images of rats' hind paws at the termination showed that HFS in the CAP-Vehicle group presented severe desquamation and redness, while forskolin treatment resulted in milder symptoms **(Fig. 5c).** Moreover, pain sensitivity was reduced in the CAP-FRSK group compared to CAP-Vehicle group **(Fig. 5d).**

HE stains of the hind paw skin revealed that the HFS model group (CAP-Vehicle) exhibited dyskeratosis (premature keratinization that did not reach the stratum corneum), disordered basal layer structure, incomplete keratinization (presence of stratum corneum cell nuclei and lack of granular layer), and immune cell infiltration. These pathological changes were alleviated in the CAP-FRSK group **(Fig. 5e)**. IHC staining of Ki67 indicated that forskolin alleviates the inhibition of keratinocyte proliferation induced by capecitabine **(Fig. 5f)**. In addition, forskolin might also exert anti-inflammatory effects by inhibiting lymphocyte and macrophage infiltration in the

236 epidermis **(Fig. 5g)**. Furthermore, TUNEL assay indicated that forskolin could alleviate
237 capecitabine-induced keratinocyte apoptosis **(Fig. 5h).**
238 In the Balb/c mice model, forskolin also slowed HFS progression, with a Grade 2
239 incidence of 50% (n=10, one death on day 11) in the CAP-Vehicle group compared to
240 0% (n=10) in the CAP-FRSK group at the end of the experiment, but spontaneous
241 remission of HFS was observed over time **(Fig. S3, A and B).** Forskolin treatment
242 significantly alleviated HFS symptoms on Babl/c mice, including scaling, redness,
243 swelling, and pain **(Fig. S3, C and D).**
244 In conclusion, these findings indicate that forskolin has considerable potential in
245 mitigating capecitabine-induced HFS.

246 6. Forskolin mitigates 5-FU effects via the ATF4-eIF2α-IκB 247 signaling pathway

248 Our in vivo and in vitro experiments demonstrated that forskolin reverses 5-FU toxicity
249 and alleviates HFS induced by capecitabine. However, the precise mechanism by which
250 forskolin mediates 5-FU detoxification through ATF4 induction remains unclear.
251 ATF4 has two classical functions[28]. First, as a key downstream effector of the
252 integrated stress response (ISR), ATF4 enhances the transcription of various stress-
253 response proteins to respond to the upregulated p-eIF2α. Second, as a negative feedback
254 regulator of ISR, ATF4 dephosphorylates p-eIF2α by upregulating GADD34.
255 Studies have shown[23] that forskolin-induced ATF4 could dephosphorylate p-eIF2α,
256 which is also verified on HaCaT in our results **(Fig. 6a, b)**. In addition, forskolin

treatment failed to increase the transcription of most genes downstream of ATF4 except *GRP78* and *P16*, but the protein levels of both genes remained unchanged **(Fig. S4)**. This evidence indicated that forskolin-induced ATF4 exerts function through the second pathway but not the first. Several studies have shown that inhibition of p-eIF2α exhibits a cellular protective effect[29-31]. Therefore, the aforementioned evidence suggests that forskolin may reverse 5-FU toxicity through dephosphorylating p-eIF2α. To investigate how ATF4/eIF2α mediates 5-FU detoxification, we performed GO enrichment analysis on Library-CR-N where ATF4 was identified. This analysis revealed enrichment in the "negative regulation of NF-κB pathway" **(Fig. 6c)**, suggesting that inhibition of the NF-κB pathway may reduce 5-FU toxicity to HaCaT cells. In addition, RNA-seq of *ATF4*-knockdown HaCaT cells confirmed that differentially expressed genes were enriched in the NF-κB pathway **(Fig. S5)**, supporting the hypothesis that ATF4 regulates the NF-κB pathway in HaCaT cells to reverse 5-FU toxicity. Furthermore, elevated p-eIF2α levels are known to induce inflammation by activating NF-κB[32], which is connected with impaired IκB expression[33]. This evidence suggests us to investigate the effects of forskolin on the ATF4-eIF2α-IκB pathway. Forskolin was found to increase IκB expression in rat skin tissues **(Fig. 6d)**. At the same time, the knockdown of *ATF4* attenuated the upregulation of IκB induced by forskolin **(Fig. 6e)**, indicating that forskolin's effect on IκB could be mediated through ATF4. Additionally, overexpression of *ATF4* successfully replicated forskolin's effects, including downregulated p-eIF2α and upregulated IκB **(Fig. 6f)**.

In summary, forskolin-induced ATF4 decreases p-eIF2α level through the negative

feedback pathway of ISR, leading to increased IκB expression **(Fig. 6g)**. Forskolin's effects on IκB were believed to derive from enhanced global translation[34]. Upregulated IκB may subsequently regulate survival, proliferation, inflammation, and other phenotypes by inhibiting the NF-κB pathway.

7. Topical forskolin treatment does not affect the anti-tumor efficacy of capecitabine

Although forskolin is designed to be administrated topically, as an adjuvant drug for chemotherapy, it necessitates concomitant administration with capecitabine. This may compromise the anti-tumor efficacy of capecitabine by triggering adverse drug-drug interactions. Therefore, we investigated the impact of local forskolin treatment on the anti-tumor efficacy of capecitabine.

We established a subcutaneous tumor-bearing nude mouse model using the human colorectal cancer cell line HCT116. When tumor volumes reached approximately 150 mm^3, capecitabine treatment was initiated, alongside the topical application of either forskolin ointment (CAP-FRSK) or its vehicle (CAP-Vehicle). Throughout the study, no significant differences in body weight were observed between the two groups **(Fig. 7a)**, suggesting that topical forskolin might not cause systemic metabolic changes.

Moreover, forskolin had no significant effect on the tumor growth inhibition induced by capecitabine **(Fig. 7b)**. By the end of the experiment, capecitabine significantly reduced tumor volume and weight, and these effects were not influenced by forskolin treatment **(Fig. 7c, d).**

300 These findings suggest that topical forskolin treatment does not impair the anti-tumor
301 efficacy of capecitabine, supporting its potential use as a safe adjuvant drug of
302 capecitabine.

303 Materials and Methods

304 1. Cell culture

305 HaCaT cells were cultured in DMEM supplemented with 10% fetal bovine serum (FBS)
306 and 1% penicillin-streptomycin in a humidified incubator at 37°C and 5% CO_2.
307 ***LDH Assay:*** HaCaT cells were plated at 8,000 cells per well in 96-well plates. Once
308 adherent, cells were treated with 20 μM 5-fluorouracil (5-FU) together with various
309 concentrations of forskolin. After 24 hours, the culture supernatant was collected, and
310 lactate dehydrogenase (LDH) activity was measured according to the manufacturer's
311 protocol (Promega). Absorbance was recorded at 490 nm to assess cell membrane
312 integrity and cytotoxicity.
313 ***CCK-8 Assay:*** HaCaT cells were plated at 8,000 cells per well in 96-well plates and
314 required adherent. Cells were subsequently exposed to 20 μM 5-FU, together with
315 gradient concentrations of forskolin. After 24 hours, CCK-8 reagent was added, and
316 absorbance at 450 nm was measured to determine cell viability. For determination of
317 IC_{50} changes, cells were exposed to a series of 5-FU concentrations for 24 hours, with
318 or without 50 μM forskolin added. IC_{50} values were calculated with GraphPad Prism.
319 ***Cell Cycle Analysis:*** HaCaT cells were plated at 3×10^5 cells per well in 6-well plates
320 and allowed to adhere. Cells were then treated with solvents (NC group), 20 μM 5-FU

321 (5-FU group), 50 μM forskolin (FRSK group), or a combination of 5-FU and forskolin
322 (5-FU+FRSK group). After 24 hours, cells were collected, fixed, and stained with
323 propidium iodide (PI). Finally, cell cycle distribution was analyzed by flow cytometry.
324 ***Apoptosis Assay:*** HaCaT cells were plated at 3×10^5 cells per well in 6-well plates and
325 allowed to adhere. Cells were treated with solvents, 40 μM 5-FU, 50 μM forskolin, or
326 a combination of 5-FU and forskolin. After 12 hours, cells were collected, washed, and
327 stained with Annexin V/PI (Beyotime) according to the manufacturer's protocol. Finally,
328 apoptotic and necrotic cells were quantified using flow cytometry.

329 2. Cell lines construction

330 Lentiviral particles were packaged with Lentiviral Packaging Kit (Genomeditech),
331 incorporating the following plasmids: Human *ATF4* knockdown plasmid (shRNA-
332 ATF4, GTTGGTCAGTCCCTCCAACAA), Human *ATF4* knockout plasmid (sgRNA-
333 ATF4, caccg-CCACTCACCCTTGCTGTTGT), and Human *ATF4* overexpression
334 plasmid (over-ATF4, NM_001675.4), along with their respective negative control
335 plasmids. The lentiviruses transduction was performed on HaCaT cells for 24 hours in
336 the presence of 8 μg/mL polybrene. Subsequently, the infected cells were selected out
337 with 2 μg/mL puromycin for 48 hours and then cultured in DMEM containing 0.5
338 μg/mL puromycin for expansion. Finally, the stable HaCaT cell lines with *ATF4*
339 knockdown, *ATF4* knockout, and *ATF4* overexpression were successfully established.

340 ## 3. Western blot analysis

341 Tissue or cell samples were lysed with RIPA buffer containing phosphatase inhibitors
342 and 1 mM PMSF. Protein extracts were quantified using BCA protein assay kit and then
343 heated at 100°C for 10 minutes with loading buffer. Proteins were separated by SDS-
344 PAGE and subsequently transferred onto a PVDF membrane using the wet transfer
345 method. The membranes were blocked at room temperature for 1 hour in 5% bovine
346 serum albumin (BSA) prepared in Tris-buffered saline with 0.1% Tween-20 (TBST).
347 Following blocking, the membrane was incubated with the following primary
348 antibodies overnight at 4 ℃: anti-ATF4 (PTG, 10835-1-AP), anti-eIF2α (Abcam,
349 ab169528), anti-p-eIF2α (MCE, HY-P80811), anti-MEK (PTG, 11049-1-AP), anti-p-
350 MEK (PTG 28955-1-AP), anti-ERK1/2 (PTG, 11257-1-AP), and anti-p-ERK1/2 (PTG,
351 28733-1-AP). The membrane was then incubated with secondary antibodies at room
352 temperature for 1 hour. After washed with TBST, protein bands were visualized with
353 chemiluminescence using Super Singal West FemtoMaximum Sensitivity Substrate
354 (Thermo Scientific). Finally, protein expression levels were evaluated by band intensity.

355 ## 4. RT-qPCR analysis

356 Total RNA was extracted from HaCaT cells using a TRIzol Reagent (YaMei) according
357 to the manufacturer's instructions. RNA quality and concentration were determined
358 using NanoDrop spectrophotometer. cDNA was synthesized using ReverTra Ace qPCR
359 RT Master Mix (TOYOBO, FSQ-301) with 50 ng/μL of total RNA concentration. RT-
360 qPCR was performed using qPCR SYBR Green Master Mix (YEASEN). Relative

361 mRNA expression level was analyzed using $2^{(-\Delta\Delta CT)}$, with GAPDH as the internal
362 reference gene. The primer sequences are listed in **Table S6**.

363 5. Animal models

364 ***HFS Model on SD Rats:*** female SD rats (6-8 weeks old) were randomly assigned to
365 three groups. Rats were gavaged daily with capecitabine (4000 mg/kg per day or its
366 vehicle (castor oil: ethanol: water, 1:1:1). After gavage, rats were restrained, and their
367 hind paws were treated topically with either a treatment gel containing 10% forskolin
368 or a vehicle gel. The gel was applied for 4 hours and then removed to prevent accidental
369 ingestion. Grouped as follows: 1) Control group (n=6) gavaged with solvent and treated
370 with vehicle gel; 2) CAP + Vehicle group (n=12) gavaged with capecitabine and treated
371 with vehicle gel; 3) CAP + FRSK group (n=12) gavaged with capecitabine and treated
372 with 10% forskolin gel. The progression of HFS was assessed daily based on paw skin
373 changes by at least two researchers. The HFS model on rats could be evaluated as Grade
374 0 (normal), Grade 1 (slight desquamation or dry lines), and Grade 2 (peeling or
375 erythema with slight desquamation). The Von Frey Filaments was used to test
376 mechanical pain threshold of rats' hind paws, recording the maximum force eliciting a
377 withdrawal response every 7 days. The whole experiment lasted approximately 5 weeks.
378 ***HFS Model on BALB/c Mice:*** Female BALB/c mice (6-8 weeks old) were randomly
379 divided into three groups. Mice were gavaged daily with capecitabine (1000 mg/kg per
380 day) or its vehicle (5% v/v gum Arabic solution, citrate buffer pH 6.0). Their hind paws
381 were treated with either a treatment gel containing 10% forskolin or a control gel for 4

382 hours. Grouped as follows: 1) Control group (n=10); 2) CAP + Vehicle group (n=10);
383 3) CAP + FRSK group (n=10). The progression of HFS was evaluated and recorded
384 daily as Grade 0 (normal), Grade 1 (slight dry lines), and Grade 2 (desquamation,
385 erythema, or swelling). Paw withdrawal responses of hind paws to pinprick stimulation
386 were assessed every 3 days. The whole experiment lasted approximately 2 weeks.
387 ***Subcutaneous Tumor Bearing Model on Nude Mice:*** Female nude mice (6-8 weeks
388 old) were injected subcutaneously with HCT116 human colorectal cancer cells (5×10^6
389 cells) mixed with matrigel. The experiment was started as the average tumor volume
390 reached approximately 150 mm^3. Mice were randomly assigned to three groups and
391 gavaged daily with capecitabine (180 mg/kg) or its vehicle (5% v/v gum Arabic solution,
392 citrate buffer pH 6.0). After gavage, their hind paws were treated with either a treatment
393 gel containing 10% forskolin or a control gel for 4 hours. Grouped as follows: 1)
394 Control group (n=6); 2) CAP + Vehicle group (n=6); 3) CAP + FRSK group (n=6).
395 Tumor length (L) and width (W) were measured every 2 days, and tumor volume (V)
396 was calculated based on $V=(L\times W^2)/2$. The experiment was discontinued when tumor
397 volume reached approximately 1500 mm^3, and the tumors were subsequently excised,
398 photographed, and weighed.

399 6. Histology

400 Rats' hind paw skin was collected and fixed in 4% paraformaldehyde (PFA) for at least
401 48 hours. The tissues were embedded in paraffin and sectioned at 4 μm thickness. The
402 sections were subjected to hematoxylin and eosin (HE) staining and

403 immunohistochemistry (IHC) staining. The IHC staining utilized the following
404 antibodies: CD3, CD68, Ki67. Apoptosis was evaluated using a TUNEL assay kit
405 (Beyotime) following the manufacturer's instructions.

406 7. Statistical analysis

407 All data in this study was performed with GraphPad Prism 8.0.1. The Significance of
408 difference between two groups was analyzed by Student's t test (unpaired, two-tailed).
409 For the data with more than two groups, one-way ANOVA was performed. The Error
410 bar was presented as the mean ± standard error of mean (SEM). $P<0.05$ was
411 considered as significant (ns, $P>0.05$; *, $P<0.05$; **, $P<0.01$; ***, $P<0.001$).
412

Discussion

This study introduces a dual-filter target screening strategy to minimize experimental validation efforts by integrating experimentally validated targets from the literature to filter HTS outputs. Subsequently, we applied this strategy to the identification of targets for drugs alleviating HFS, demonstrating its potential to enhance target screening efficiency. Under this strategy, we identified ATF4 as a key target regulating 5-FU toxicity. Forskolin, an ATF4 inducer, was then found to significantly detoxify 5-FU and alleviate HFS.

Crucially, when applied to HFS, our strategy narrowed 127 initial candidates derived from CRISPR/Cas9 screening down to 2 high confidence targets, reducing target validation burden by 98% compared with conventional HTS.

This strategy is also applicable to target identification in the context of various research objectives. When the number of candidate targets obtained through the screening process remains extensive, the optimal target can be determined by integrating the rankings derived from the two screening methods. Compared to the approach introduced by Gogleva et al.[12], our screening system is more straightforward and has fewer limitations in application scenarios while preserving robust target identification capabilities. However, in cases where the literature in the field of study is limited, this approach may fail to identify relevant targets or overlook potentially high-priority novel targets. In such scenarios, leveraging literature from related research fields may provide valuable insights for target identification.

Beyond establishing a universally applicable target screening method, this study has

generated clinically meaningful and academically valuable findings in its application to HFS. Our results not only identified an alternative strategy for the management of HFS but also provided new insights into understanding and modulating the toxicity associated with 5-FU.

According to our results, forskolin is determined to detoxify 5-FU through ATF4/eIF2α/IκB. This indirectly verifies the view proposed by Gameiro P A [32]that high levels of p-eIF2α activate NF-κB and promote inflammation, and to a certain extent supports the widely reported anti-inflammatory effect of forskolin [35,36]. However, the ATF4 expression-mediated 5-FU detoxification signaling pathway identified in this study differs from the widely reported ATF4-induced signaling pathways. This discrepancy may be attributed to the fact that forskolin induces ATF4 via a non-stress signaling pathway[37,38]. In the future, the findings of this study may stimulate further research on forskolin and provide insights into investigations aimed at overcoming 5-FU resistance. However, since the chemotherapy adjuvant drug that was discovered by targeting chemotherapy toxicity has to be administered locally to avoid compromising anti-tumor efficacy, forskolin may only be appropriate for localized treatments. Future research could focus on improving the tissue specificity of the chemotherapy adjuvant drug by integrating information from additional databases, thereby enabling systemic administration for side effects without negatively impairing the anti-tumor efficacy.

Figures

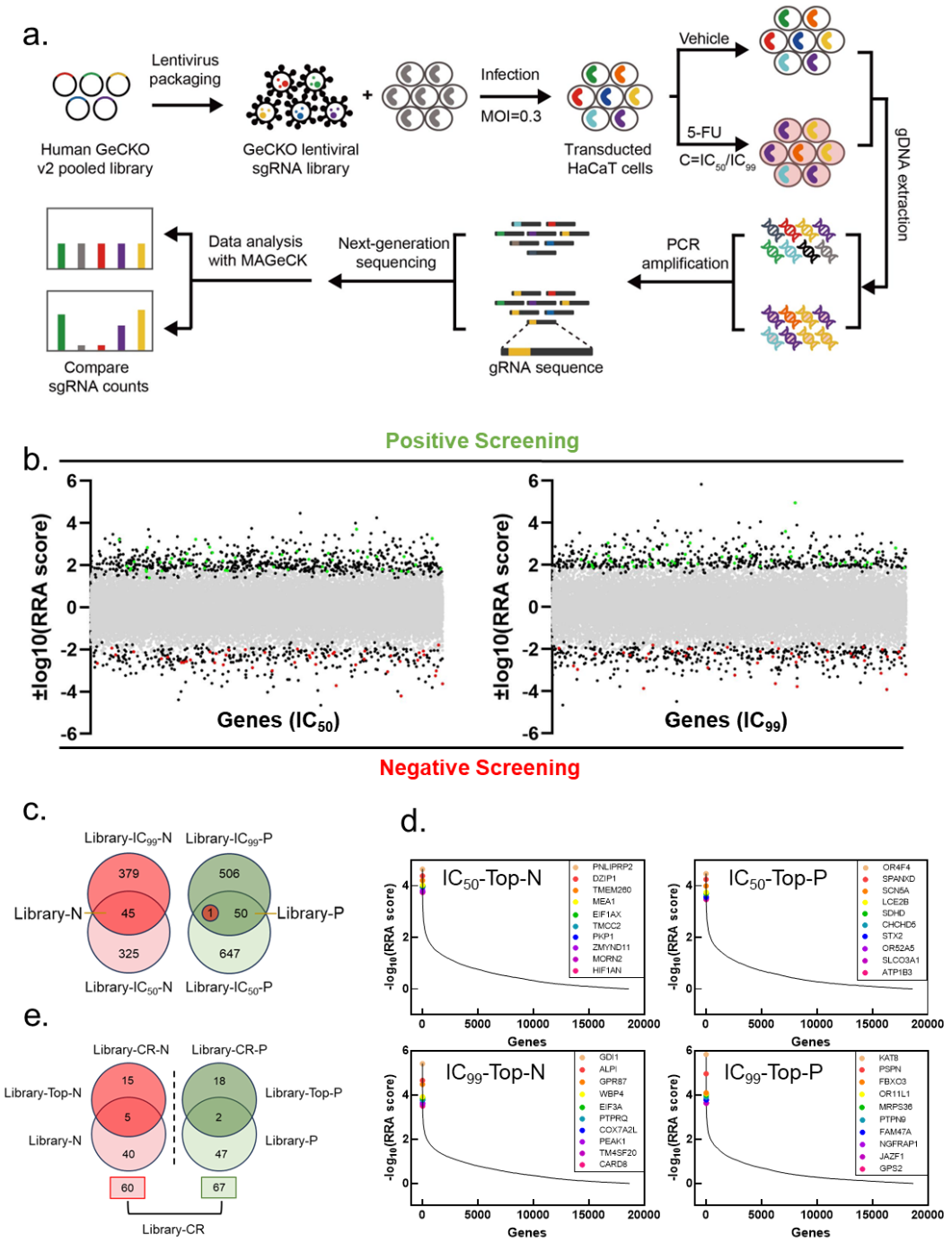

Fig 1 Genome-wide CRISPR/Cas9 screening results (a) Experimental workflow of genome-wide CRISPR/Cas9 screening. (b) RRA score distribution of Library-N and Library-P. (c) Definitions of Library-N and Library-P. (d) Top 10 targets screened by genome-wide CRISPR/Cas9. (e) Definition of Library-CR.

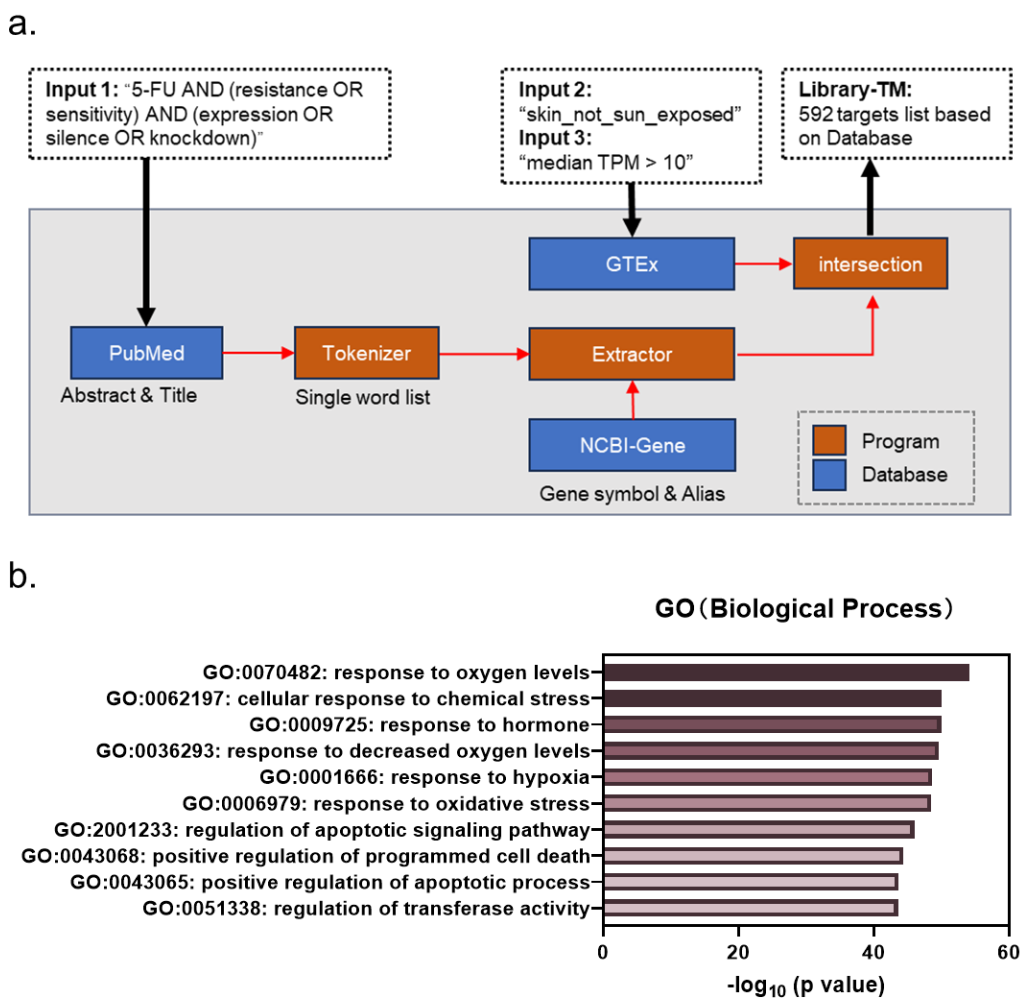

Fig 2 Text mining screening results. (a) Workflow of text mining screening. (b) GO enrichment analysis of Library-TM.

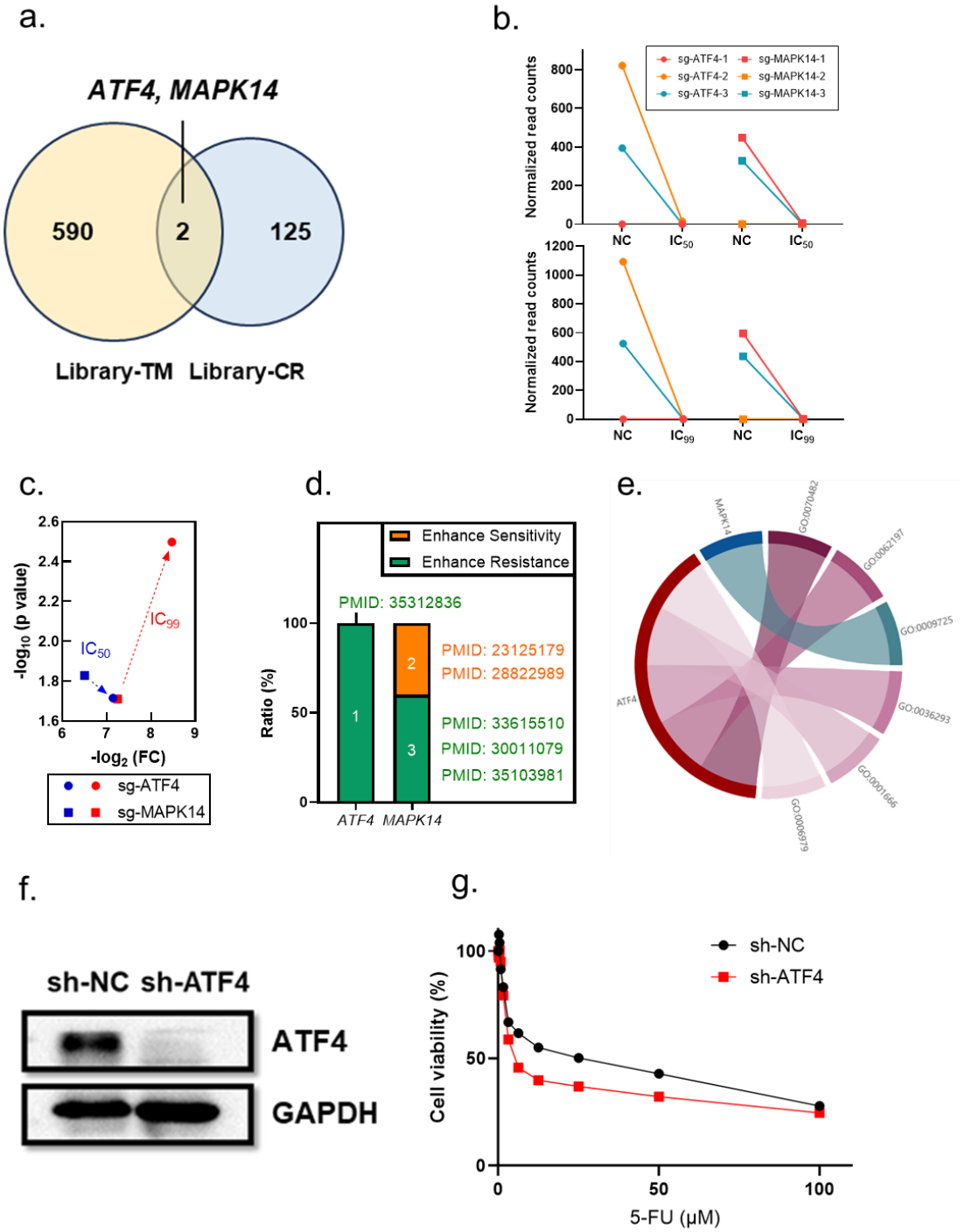

Fig 3 Targets identification process. (a) *ATF4* and *MAPK14* are identified through combining CRISPR/Cas9 and text mining screening. (b) *ATF4* knockout has a stronger influence on normalized sgRNA counts. (c) Comparison of the changes in sgRNA counts and its statistical significance (d) The reported regulatory ability on 5-FU toxicity of *MAPK14* shows poor consistency. (e) The occurrence frequencies of *ATF4* and *MAPK14* in stress-related GO terms. (f) ATF4 protein expression in the *ATF4* knockdown cell line. (g) The impact of *ATF4* knockdown on 5-FU IC_{50}

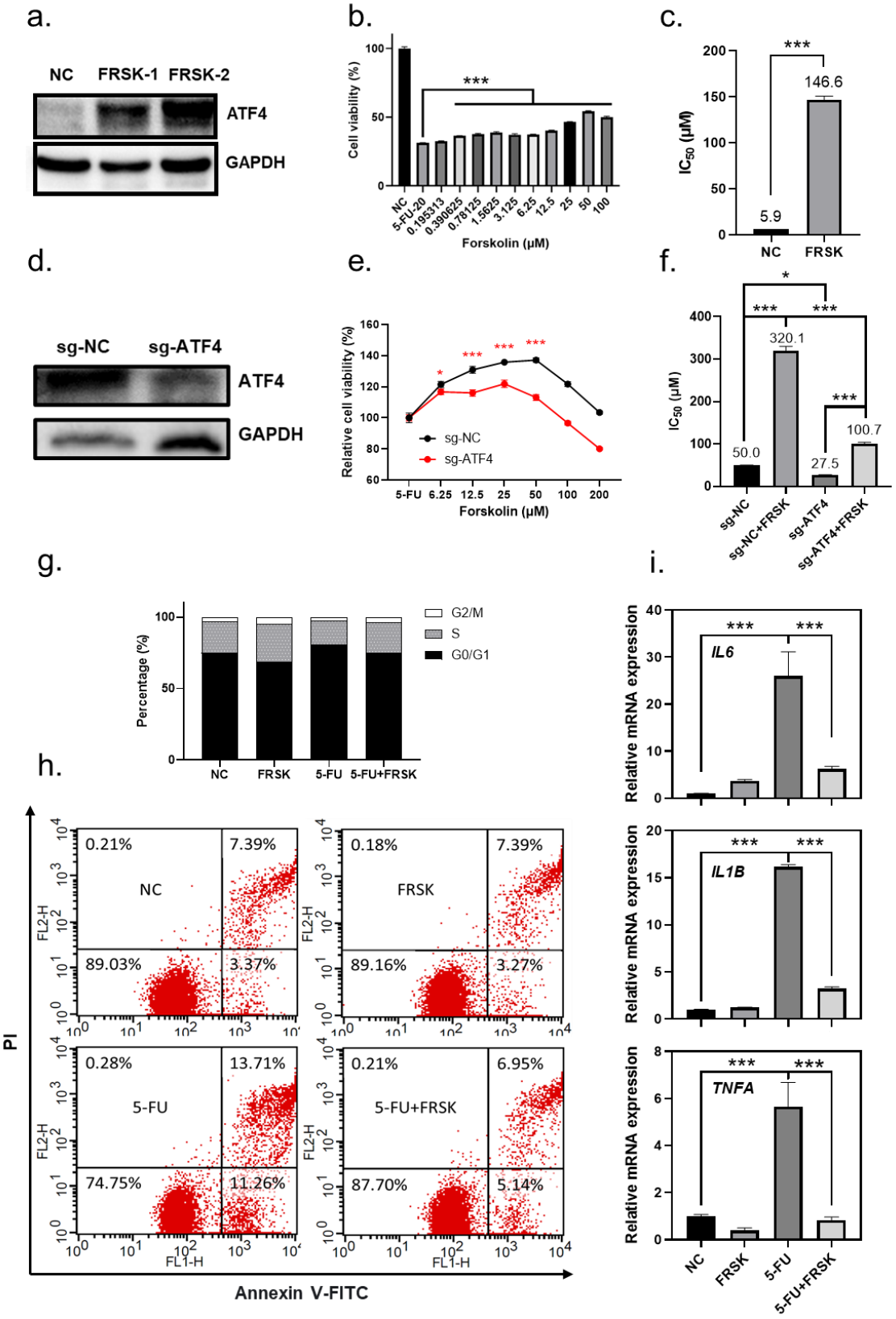

Fig 4 The efficacy of forskolin in detoxifying 5-FU evaluated on HaCaT. (a) Forskolin significantly induced ATF4 expression. (b) Forskolin alleviated 5-FU-induced cytotoxicity, and (c) increased 5-FU IC_{50}. (d), (e), (f) *ATF4* knockout impaired forskolin's ability to reverse 5-FU toxicity (g) cell cycle arrest, (h) cell apoptosis, and (i) the release of typical pro-inflammatory cytokines.

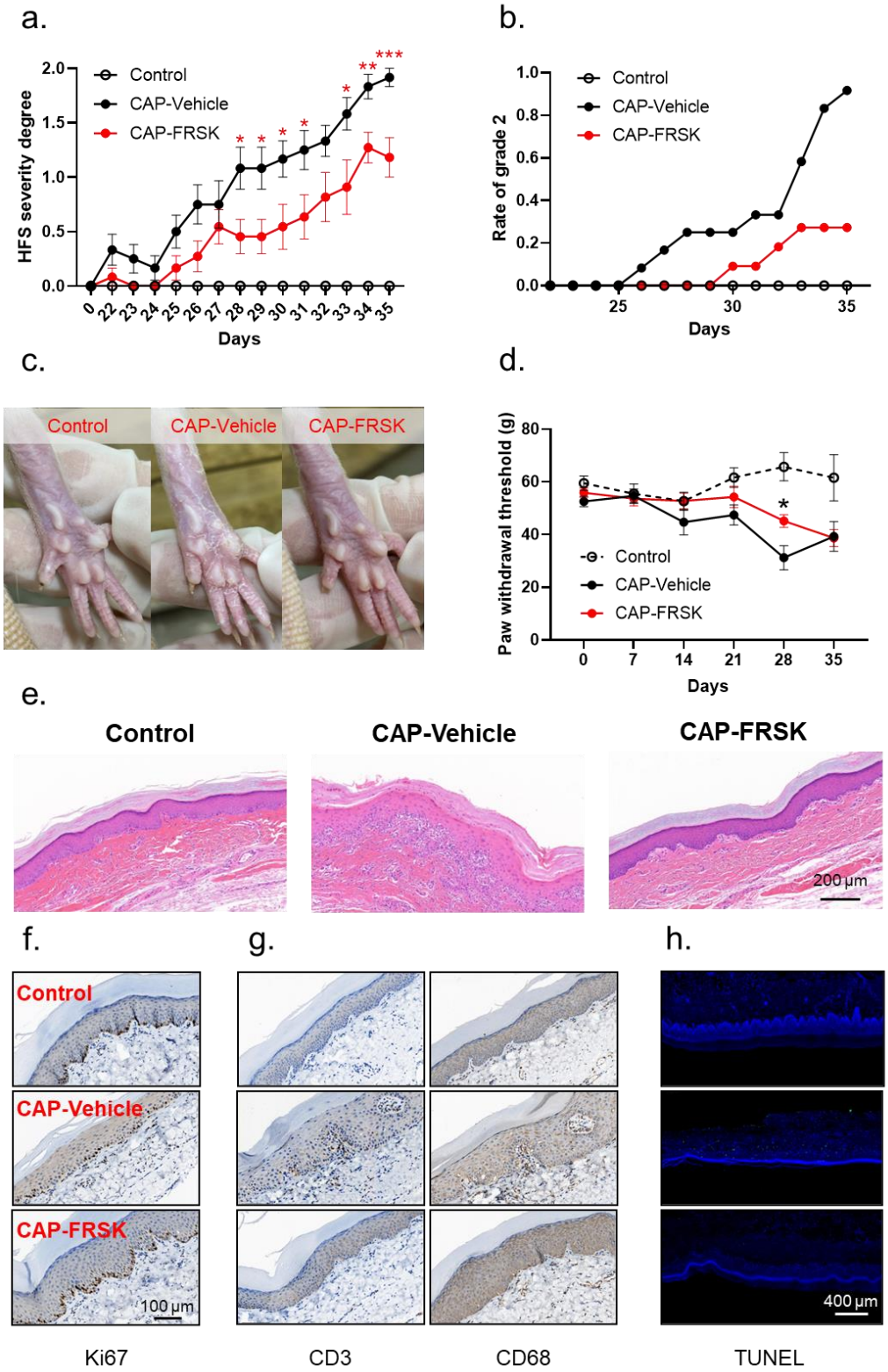

Fig 5 The efficacy of forskolin in alleviating HFS evaluated on rats. (a) Forskolin relieves the severity of HFS in rats. (b) Forskolin reduced the rate of grade 2 HFS on rats. (c) Representative images of HFS symptoms on the rats' hind paws. (d) Forskolin elevated paw withdrawal threshold. (e) HE stains images of the full-thickness skin of the rats' hind paws. (f), (g) IHC stains of Ki67, CD3 and CD68. (h) The TUNEL stains images of the rats' hind paw skin.

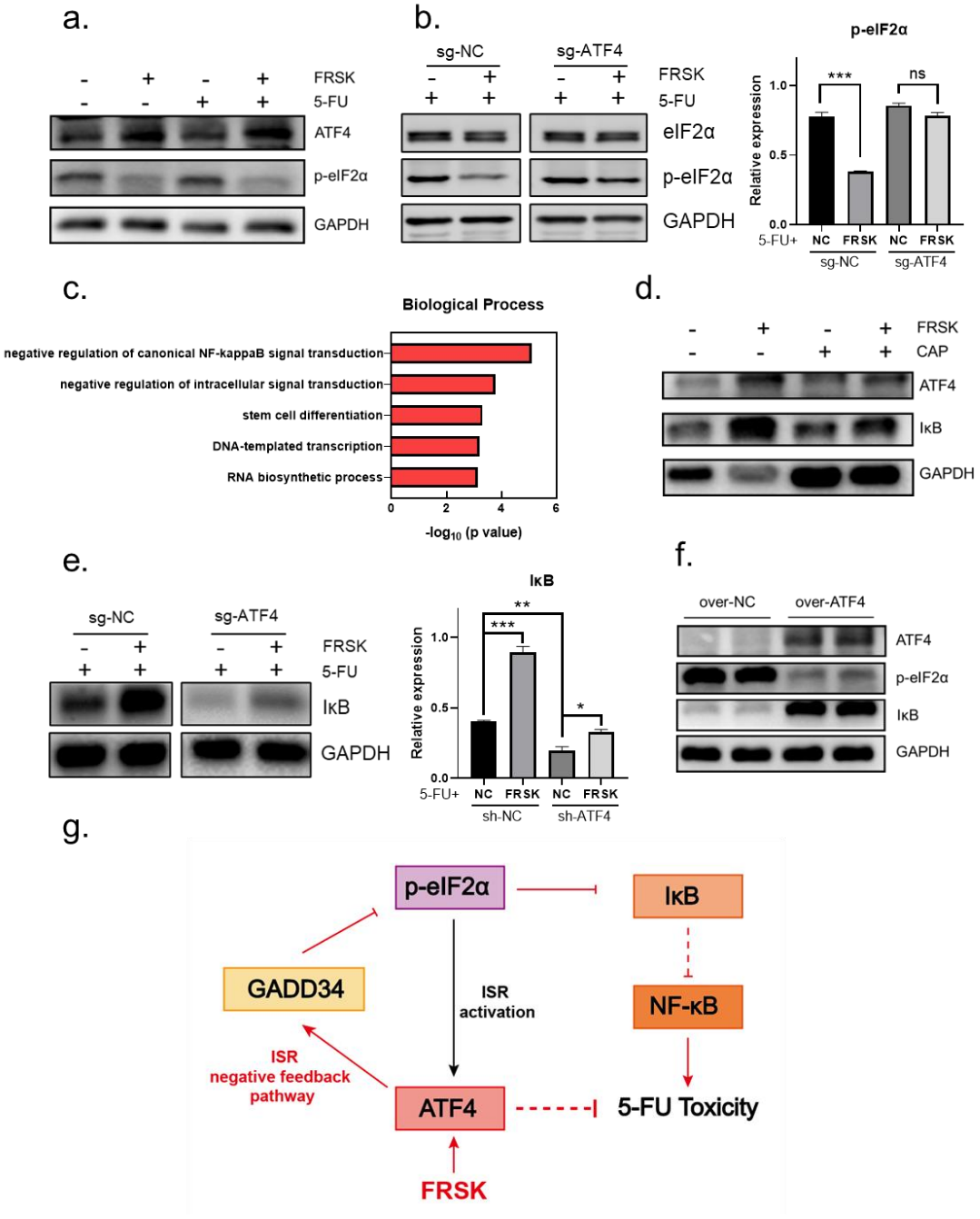

Fig 6 The biological mechanism underlying forskolin action. (a) 12 h forskolin treatment downregulated p-eIF2α in HaCaT. (b) *ATF4* knockout impaired forskolin's ability to downregulate p-eIF2α in HaCaT. (c) Genes in Library-CR-N were enriched in negative regulation of NF-κB pathway. (d) forskolin treatment upregulated IκB expression in rats' hind paw skin. (e) *ATF4* knockdown impaired forskolin's ability to upregulate IκB in HaCaT.(f) *ATF4* overexpression replicated the effect of forskolin on p-eIF2α and IκB expression in HaCaT. (g) The possible biological mechanism of forskolin to detoxify 5-FU.

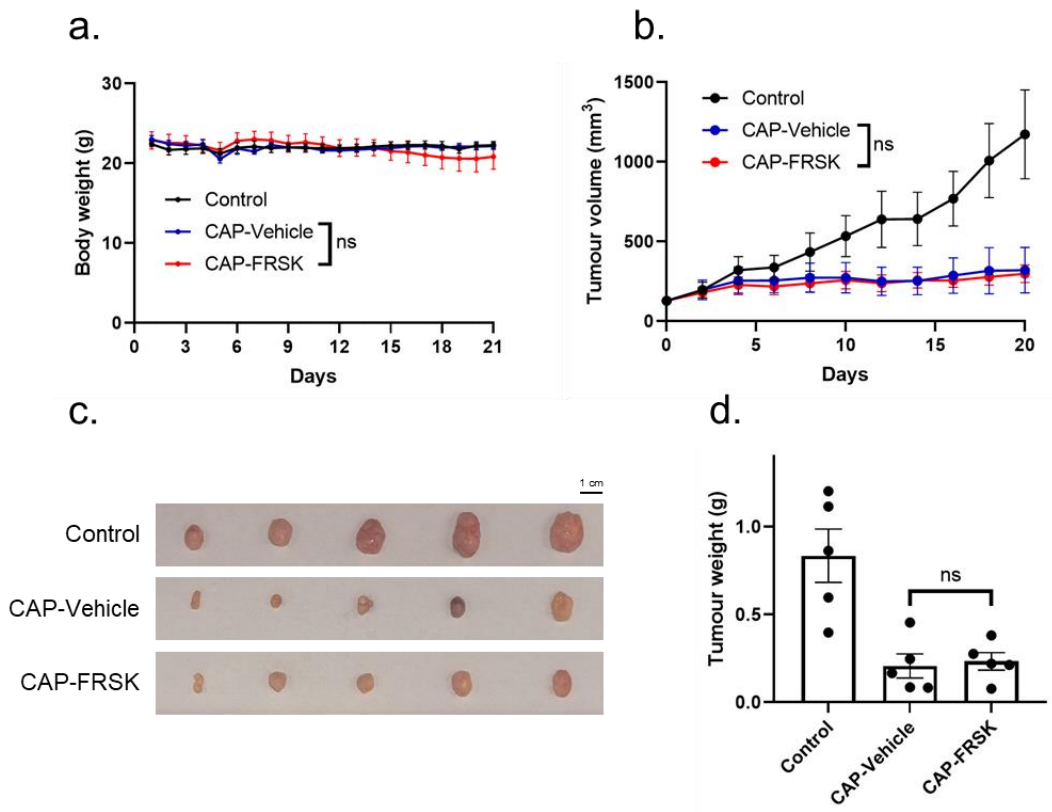

Fig 7 Effects of topical forskolin on anti-tumor efficacy of capecitabine. (a) Topical forskolin has no effect on body weight and (b) tumor volume change. (c) Comparison of tumor volume and (d) tumor weight

Reference

[1]. Kurata M, Yamamoto K, Moriarity B S, et al. CRISPR/Cas9 library screening for drug target discovery[J]. Journal of Human Genetics, 2018, 63(2): 179-186.

[2]. Zhu Q, Lin Q, Jiang Y, et al. Construction and application of the conditionally essential gene knockdown library in Klebsiella pneumoniae to screen potential antimicrobial targets and virulence genes via Mobile-CRISPRi-seq[J]. Applied and Environmental Microbiology, 2023, 89(10): e00956-23.

[3]. Jiang W, Oikonomou P, Tavazoie S. Comprehensive genome-wide perturbations via CRISPR adaptation reveal complex genetics of antibiotic sensitivity[J]. Cell, 2020, 180(5): 1002-1017. e31.

[4]. Li B, Clohisey S M, Chia B S, et al. Genome-wide CRISPR screen identifies host dependency factors for influenza A virus infection[J]. Nature communications, 2020, 11(1): 164.

[5]. Rottner A K, Ye Y, Navarro-Guerrero E, et al. A genome-wide CRISPR screen identifies CALCOCO2 as a regulator of beta cell function influencing type 2 diabetes risk[J]. Nature Genetics, 2023, 55(1): 54-65.

[6]. Sheel A, Xue W. Genomic amplifications cause false positives in CRISPR screens[J]. Cancer discovery, 2016, 6(8): 824-826.

[7]. Tian S, Qin Y, Wu Y, et al. Design, performance, processing, and validation of a pooled CRISPR perturbation screen for bacterial toxins[J]. Nature Protocols, 2024: 1-38.

[8]. Yamauchi T, Masuda T, Canver M C, et al. Genome-wide CRISPR-Cas9 screen identifies leukemia-specific dependence on a pre-mRNA metabolic pathway regulated by DCPS[J]. Cancer cell, 2018, 33(3): 386-400. e5.

[9]. Li H, Song J, He Y, et al. CRISPR/Cas9 Screens Reveal that Hexokinase 2 Enhances Cancer Stemness and Tumorigenicity by Activating the ACSL4 - Fatty Acid β - Oxidation Pathway[J]. Advanced Science, 2022, 9(21): 2105126.

[10]. Mohanty S, Mohapatra P, Shriwas O, et al. CRISPR-based kinome-screening revealed MINK1 as a druggable player to rewire 5FU-resistance in OSCC through AKT/MDM2/p53 axis[J]. Oncogene, 2022, 41(45): 4929-4940.

[11]. Pan J, Zhang M, Dong L, et al. Genome-Scale CRISPR screen identifies LAPTM5 driving lenvatinib resistance in hepatocellular carcinoma[J]. Autophagy, 2023, 19(4): 1184-1198.

[12]. Gogleva A, Polychronopoulos D, Pfeifer M, et al. Knowledge graph-based recommendation framework identifies drivers of resistance in EGFR mutant non-small cell lung cancer[J]. Nature communications, 2022, 13(1): 1667.

[13]. Degen A, Alter M, Schenck F, et al. The hand-foot-syndrome associated with medical tumor therapy–classification and management[J]. JDDG: Journal der Deutschen Dermatologischen Gesellschaft, 2010, 8(9): 652-661.

[14]. Mrozek-Orlowski M E, Frye D K, Sanborn H M. Capecitabine: nursing implications of a new oral chemotherapeutic agent[C]//Oncology nursing forum. 1999, 26(4): 753-762.

[15]. Cassidy J, Twelves C, Van Cutsem E, et al. First-line oral capecitabine therapy in metastatic colorectal cancer: a favorable safety profile compared with intravenous5-

fluorouracil/leucovorin[J]. Annals of oncology, 2002, 13(4): 566-575.

[16]. Yang B, Xie X, Wu Z, et al. DNA damage-mediated cellular senescence promotes hand-foot syndrome that can be relieved by thymidine prodrug[J]. Genes & Diseases, 2023, 10(6): 2557-2571.

[17]. Klubes P, Leyland-Jones B. Enhancement of the antitumor activity of 5-fluorouracil by uridine rescue[J]. Pharmacology & therapeutics, 1989, 41(1-2): 289-302.

[18]. Netikova I, Sedlackova E, Konopasek B, et al. Therapy of palmar-plantar erythrodysesthesia after continual fluoropyrimidin administration with 10% uridin ointment[J]. Journal of Clinical Oncology, 2009, 27(15_suppl): e20690-e20690.

[19]. Hartinger J, Veselý P, Matoušková E, et al. Local Treatment of Hand-Foot Syndrome with Uridine/Thymidine: In Vitro Appraisal on a Human Keratinocyte Cell Line HaCaT[J]. The Scientific World Journal, 2012, 2012(1): 421325.

[20]. Li H, Song J, He Y, et al. CRISPR/Cas9 Screens Reveal that Hexokinase 2 Enhances Cancer Stemness and Tumorigenicity by Activating the ACSL4-Fatty Acid β-Oxidation Pathway[J]. Advanced Science, 2022, 9(21): 2105126.

[21]. Tang S, Pollok K E, Pandya P H, et al. Genome-wide CRISPR/Cas9 screening reveals ATR as a therapeutic target that overcomes osteosarcoma chemoresistance[J]. Cancer Research, 2022, 82(12_Supplement): 3971-3971.

[22]. Jiang C, Qian M, Gocho Y, et al. Genome-wide CRISPR/Cas9 screening identifies determinant of panobinostat sensitivity in acute lymphoblastic leukemia[J]. Blood advances, 2022, 6(8): 2496-2509.

[23]. Yusta B, Baggio L L, Estall J L, et al. GLP-1 receptor activation improves β cell function and survival following induction of endoplasmic reticulum stress[J]. Cell metabolism, 2006, 4(5): 391-406.

[24]. Yoshikawa R, Kusunoki M, Yanagi H, et al. Dual antitumor effects of 5-fluorouracil on the cell cycle in colorectal carcinoma cells: a novel target mechanism concept for pharmacokinetic modulating chemotherapy[J]. Cancer research, 2001, 61(3): 1029-1037.

[25]. Nita M E, Nagawa H, Tominaga O, et al. 5-Fluorouracil induces apoptosis in human colon cancer cell lines with modulation of Bcl-2 family proteins[J]. British journal of cancer, 1998, 78(8): 986-992.

[26]. Rapa S F, Magliocca G, Pepe G, et al. Protective effect of pomegranate on oxidative stress and inflammatory response induced by 5-fluorouracil in human keratinocytes[J]. Antioxidants, 2021, 10(2): 203.

[27]. Gressett S M, Stanford B L, Hardwicke F. Management of hand-foot syndrome induced by capecitabine[J]. Journal of Oncology Pharmacy Practice, 2006, 12(3): 131-141.

[28]. Singleton D C, Harris A L. Targeting the ATF4 pathway in cancer therapy[J]. Expert opinion on therapeutic targets, 2012, 16(12): 1189-1202.

[29]. Kim H J, Raphael A R, LaDow E S, et al. Therapeutic modulation of eIF2α phosphorylation rescues TDP-43 toxicity in amyotrophic lateral sclerosis disease models[J]. Nature genetics, 2014, 46(2): 152-160.

[30]. Halliday M, Radford H, Zents K A M, et al. Repurposed drugs targeting eIF2α-P-mediated translational repression prevent neurodegeneration in mice[J]. Brain, 2017,

140(6): 1768-1783.

[31]. Lee S, Jee H Y, Lee Y G, et al. PKR-mediated phosphorylation of eIF2a and CHK1 is associated with doxorubicin-mediated apoptosis in HCC1143 triple-negative breast cancer cells[J]. International Journal of Molecular Sciences, 2022, 23(24): 15872.

[32]. Gameiro P A, Struhl K. Nutrient deprivation elicits a transcriptional and translational inflammatory response coupled to decreased protein synthesis[J]. Cell reports, 2018, 24(6): 1415-1424.

[33]. Deng J, Lu P D, Zhang Y, et al. Translational repression mediates activation of nuclear factor kappa B by phosphorylated translation initiation factor 2[J]. Molecular and cellular biology, 2004, 24(23): 10161-10168.

[34]. Wek R C. Role of eIF2α kinases in translational control and adaptation to cellular stress[J]. Cold Spring Harbor perspectives in biology, 2018, 10(7): a032870.

[35]. Chen Y, Wen J G, Feng J J, et al. Forskolin attenuates the NLRP3 inflammasome activation and IL-1β secretion in human macrophages[J]. Pediatric Research, 2019, 86(6): 692-698.

[36]. Chiadak J D, Arsenijevic T, Verstrepen K, et al. Forskolin Inhibits Lipopolysaccharide-Induced Modulation of MCP-1 and GPR120 in 3T3-L1 Adipocytes through an Inhibition of NFκB[J]. Mediators of inflammation, 2016, 2016(1): 1431789.

[37]. Wek R C. Role of eIF2α kinases in translational control and adaptation to cellular stress[J]. Cold Spring Harbor perspectives in biology, 2018, 10(7): a032870.

[38]. Luo S, Baumeister P, Yang S, et al. Induction of Grp78/BiP by translational block: activation of the Grp78 promoter by ATF4 through an upstream ATF/CRE site independent of the endoplasmic reticulum stress elements[J]. Journal of Biological Chemistry, 2003, 278(39): 37375-37385.